Wet Friction-Elements Boundary Friction Mechanism and Friction Coefficient Prediction

WANG Yanzhong[a], WEI Bin[a], WU Xiangyu[a]

[a] School of Mechanical Engineering, Beijing University of Aeronautics and Astronautics, Beijing, China

A B S T R A C T

The friction mechanism for the boundary friction course of friction elements engagement was explicitly expressed. The boundary friction model was built up by the surface topography. The model contained the effect of boundary film, adhesion, plough and lubrication. Based on the model, a coefficient for weakening plough for the lubrication was proposed. The modified model could fit for the working condition of wet friction elements. The friction coefficient as a function curve of rotating speed could be finally obtained by the data k and s/s_m. The method provides a well interpretation of friction condition and friction coefficient prediction and the agreement between theoretical and experimental friction coefficients is reasonably good.

1. INTRODUCTION

In 1920s, the phrase 'boundary lubrication' was first introduced by Hardy [1]. He proposed that when the metallic surfaces in relative motion are separated by a thin lubricant film, thus, friction is reduced due to the physical and chemical interactions. Early investigations on boundary lubrication were primarily focused on the variables as molecular structure of the lubricant, environmental conditions, interfacial temperature physisorption and chemisorption of the solid surfaces. One of the earliest models of friction in boundary lubricated sliding is proposed by Bowden et al [2,3]. In the models, friction between lubricated sliding surfaces is attributed to adhesion at solid-to-solid contacts and shearing of the lubricant film. Komvopoulos et al [4], investigated the primary friction mechanisms in boundary lubricated sliding, and

confirmed that plowing is the key mechanism of friction, while adhesion between asperities and the shearing of lubricant films are generally of secondary importance. Along with the theoretical research, the experimental study has not stopped. Most of the experiments were finished with the help of surface force testing device [5-8]. Original researches about relative speed to boundary friction coefficient were concentrating on lower velocity [9,10] and the objects were often aimed at the paper based friction elements of the civil vehicle [11,12].The main purpose of this paper is to investigate the friction mechanism of sintered material and establish a boundary friction model including the effect together with plough, boundary film, adhesive contact and lubrication, which can serve for the sintered material in tracked vehicle.

2. BOUNDARY FRICTION MODEL

Typical friction mechanism is shown in Fig. 1. In this friction theory, some of the asperities boundary film would rupture due to the excessive pressure (Fig.1(S)). The bearing area B is mainly boundary friction. The boundary film bears the most of the load. The region C is the pores formed by the cavity between asperities contact. The region F is the hydrodynamic lubrication bearing area. Along with the relative speed slowing down the effect of squeezing and hydrodynamic is gradually weakened. If the liquid affect is neglected, the friction force F can be expressed as equation 1:
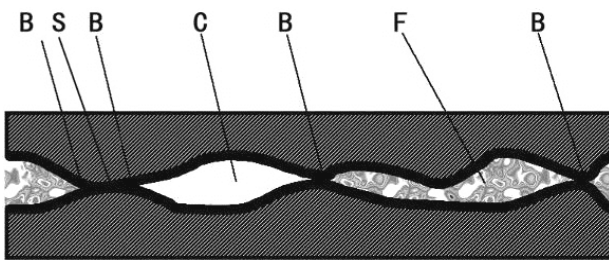

Fig. 1. Boundary lubrication model.

$$F=A_r[\alpha \cdot s_m+(1-\alpha)s_l]+F_f \qquad (1)$$

Where A_r is the real area between the two surfaces; α is the proportion of solid contact area A_s in real contact area A_r, $\alpha=A_s/A_r$. s_m is the shear strength of adhesive contact. s_l is the shear strength of boundary film. F_f is the plough force. When $\alpha=0$, it implies that the whole interface is covered by boundary film. In the real contact area A_r, αA_r is the solid direct contact and $(1-\alpha)A_r$ is separated by the boundary film. This friction model is made up by the effect of solid friction, boundary friction, and plough force. In some condition, the plough force can be neglected. Thus, equation 1 can be derived as:

$$F=A_r[\alpha \cdot s_m+(1-\alpha)s_l] \qquad (2)$$

If the load $N=A_r\sigma_s$, where σ_s is the compressive yield strength of softer material, the boundary friction coefficient could be derived via equation 2.

$$f_M = \frac{F}{N} = \alpha \frac{s_m}{\sigma_s}+(1-\alpha)\frac{s_l}{\sigma_s} \qquad (3)$$

Where f_M is synthesize friction coefficient.

If the solid friction coefficient is defined as $f_s=s_m/\sigma_s$, the boundary friction coefficient is defined as $f_b=s_l/\sigma_s$ when the interface is fully covered by the boundary film, the equation 3 can be derived as

$$f_M=\alpha f_s+(1-\alpha)f_b \qquad (4)$$

In boundary friction state, when the boundary film can play an advantage effect to lubrication, α is a relatively small value. The friction force F can be approximated as

$$F=A_r s_l \; ; \; f_M=s_l \sigma_s \qquad (5)$$

Where σ_s is the compression yield strength.

In Bowen's model [3], the body and boundary film shear strength can be obtained by experiments, however, the parameter α is difficult to determine so that the friction coefficient cannot be acquired by the equation 2. In addition, the plough effect is neglected in this model, but it is unreasonable for sintered materials friction elements in which there are lots of hard points existed. In W. Scott's experiments [13], the value calculated by the equation 4 is improper for the wet friction elements. The lubrication and cooling condition should be considered for predicting the boundary friction coefficient.

The massive experiments show that the changes of friction coefficient are corresponded with the friction mechanism. A realistic friction model must take account of the fundamental mechanisms of friction and lubrication at friction plates' interface. The picture for sintered bronze material in Fig. 2 was acquired by stereomicroscope. In micrometre scope, the pores and the plough could be observed. The pores could store some liquid when two surfaces were tightly compacted. There are two advantages existed. The one is that the liquid in the pores could take some heat away to bring the body temperature down. The other, it is promoting the generation of boundary film to minimize the adhesive effect. However, the adhesive phenomenon is inevitable in heavy duty condition for high-power friction elements. When the scale continually zooms in (Fig. 3), the pores are out of sight, otherwise the plough becomes more obvious mean while it is observed by the laser topography instrument that some asperities are clipped and some copper material is migrated to the counter steel

disc. These phenomena expressed that there is adhesion emerging for the heavy duty and high power friction element during the engagement.
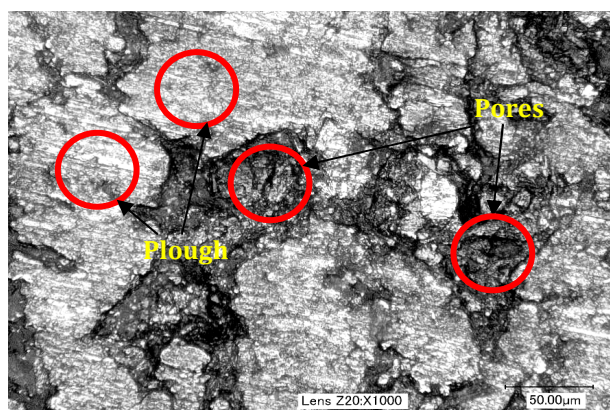

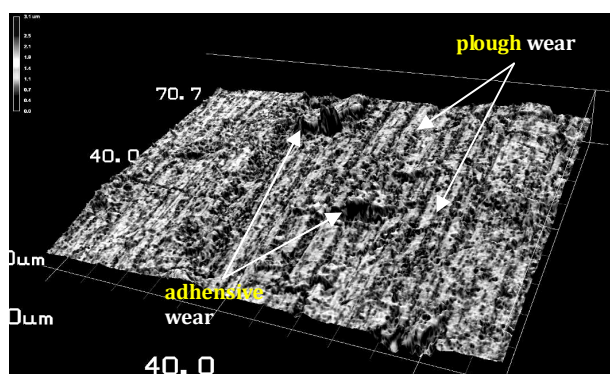**Fig. 2.** Stereomicroscope topography images.

Fig. 3. The surface topography image by laser topography instrument.

full sacle coordinate indicates:
Torque: 100 N·m   Pressure: 2 MPa
Friction coefficieng: 0.4   Rotating speed: 10000 r/min
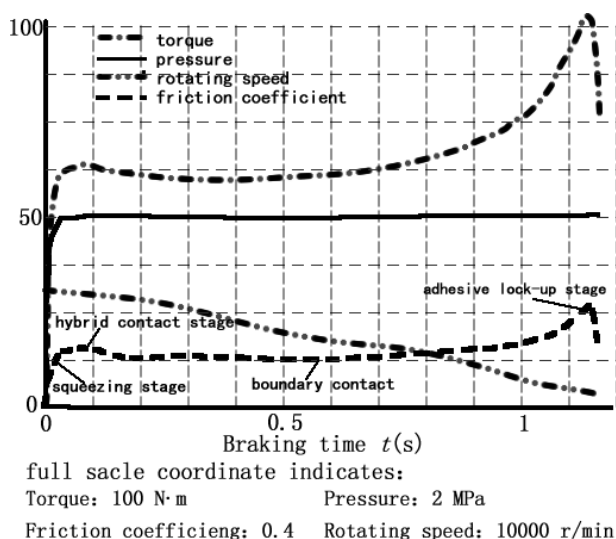
Fig. 4. SAE clutch test-bed testing friction coefficient curve.

The wet friction elements typical braking process curve is shown as Fig. 4. It shows that various parameters change with the braking time and it implies that the load controlled by

nitrogen tank is basically stable, the velocity is decreasing linearly and the toque curve has the same trend with friction coefficient curve due to the stable load. At the beginning of the brake process, the friction coefficient curve is slightly fluctuant and becomes flat subsequently. When the relative speed of the friction plates is near with each other, the friction coefficients reach the peak of the curve.

The different stages of friction can be characterized by the contact state. Four main stages may occur in brake processes. These are:

1 Lubricant film stage (Fig. 1. (squeezing stage)): the surface is separated by a continuous film of lubricant which is thicker than the roughness of the surface. There are two cases: The one is surface roughness has little influence on the lubrication; the other, the film thickness formulate should be modified by the roughness surface profile. In this stage, lubrication is essentially a mechanical process and friction is decided by the shear resistance of the lubricant film under the conditions at the interface.

2 Mixed film stage (Fig. 1. (hybrid contact stage)): the mean lubricant film thickness is about three times less than the RMS composite roughness of the surface [14]. The interface loading is shared between the pressurized lubricant film in roughness valleys and contacts at asperity peaks. In reality if the lubricant is properly formulated, actual metal-to-metal contact will not occur at asperity peaks because of the presence of tightly adhering boundary films formed as a result of chemical reaction or physical absorption of active lubricant species at the surfaces. Even though these films are very thin (of the order of the lubricant molecular size) they prevent metal-to metal contact, adhesion and pick-up during asperity collisions.

3 Boundary friction stage (Fig. 1. (boundary contact stage)): the load between the surfaces is supported purely by the contact between the rough peaks. In fact properly formulated lubricants will contain materials which will react chemically with the surface forming tightly adhering boundary lubricant films. These films have the capacity of reducing the adhesion between the surfaces. This not only reduces friction directly by reducing the shear strength of the junctions, but also, by reducing tangential

loading on the junctions and tends to suppress growth of real area of contact.

4 adhesions or partly adhesion stage (Fig. 1. (adhesive stage)): At this stage, most of the boundary film begins to crack. The asperities have bear most of the external load. The boundary friction gradually converts to adhesion friction. In this stage the relative sliding speed is small enough to neglect the effect to friction coefficient. The friction coefficient can be dramatically increased account for the conversion form kinetic friction to static friction.

The working parameters and partly experimental results are listed in Table 1 and Table 2. These data in Table 2 are the average of the 20 times results after the running in 50 hours.

Table 1. Working condition in braking process.

Nominal Pressure (MPa)	Braking Speed (r/min)	Braking inertia (kg•m²)
1	3000	30

Table 2. Experimental results.

Average friction coefficient	Max friction coefficient (lock-up)	Braking time (s)
0.053	0.11	1.2

As the boundary friction process can last for longer time and most of the heat generated in this stage, it can be more important than the other three stages. As an important stage during engagement of friction plates, the first research content is the surface topography of friction plates. In order to investigate the characteristic of boundary friction, it is necessary to simplify the surface topography. It was postulated that the asperities has the similar feature to the part of sine surface. The simplified surface can be expressed by the roughness obtained by experiments. Thus the surface equation is expressed as:

$$z = A_m \sin\left(\frac{2\pi x}{\lambda_1}\right)\sin\left(\frac{2\pi y}{\lambda_2}\right) \quad 0<x<L_x, \quad 0<y<L_y \quad (6)$$

Where the A_m is the amplitude of the sine function, λ_1 and λ_2 are the wavelength of x and y direction. The roughness can be simulated by adjusting the value of A_m. The asperities

direction and asperities density can be controlled by adjusting the λ_1 and λ_2. The surface topography is shown as Fig. 5, where dimensionless X, Y can be express as:

$$X=x/L_x, Y=y/L_y$$

Due to the existence of the lubricants, the friction force in real interface of the friction plates should including the effect of adhesion, boundary film and plough. If the asperity deformation is small enough, the sine topography can be taken place by the part of sphere [16,17]. The friction coefficient μ can be derived via the model as shown in Fig. 6.
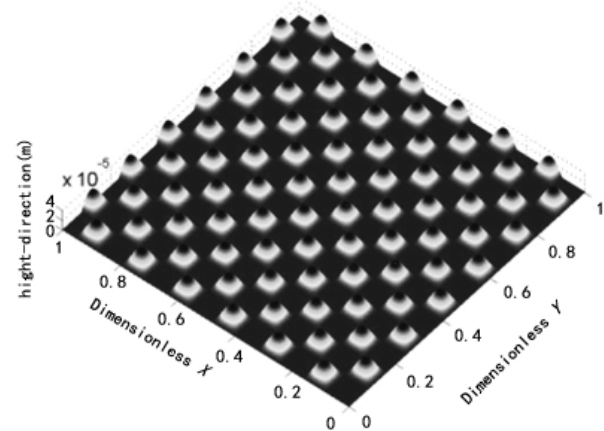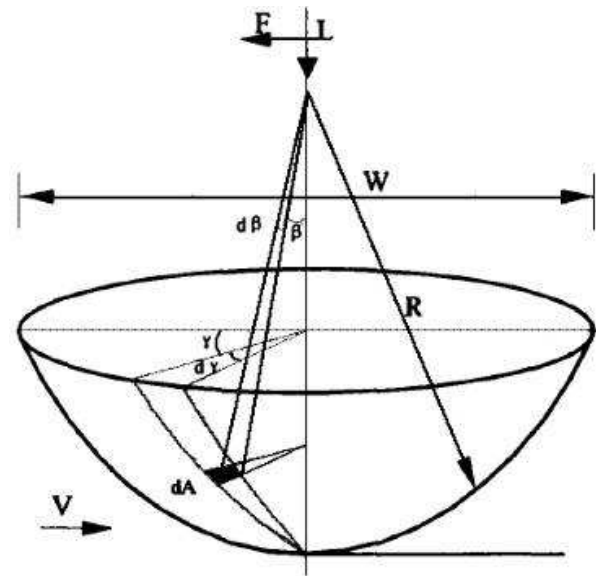

Fig. 5. Simulated surface topology.

Fig. 6. Ball micro-bulge model.

For the spherical asperity model, the normal and tangential forces, L, F, acting on an infinitesimal area, dA can be expressed as:

$$dL=p\cos\beta dA \quad (7)$$

$$dF = p\sin\beta\cos\gamma dA + s\cdot\sin\gamma dA \qquad (8)$$

Where $dA = R^2\sin\beta d\beta d\gamma$, and r is the radius of the sphere. Integrating the above two equations over the front half of the sphere where contact occurs, the process is shown as

$$L = \iint dL = \iint p\cdot\cos\beta\cdot R^2\sin\beta\cdot d\beta d\gamma$$
$$= 2pR^2\int_0^\theta \sin\beta\cos\beta d\beta\int_0^{\pi/2} dr = \frac{\pi}{2}pR^2\sin^2\theta \qquad (9)$$

It is reasonable to assume that the normal pressure p is approximately equal to the hardness, p_m of the material being plowed, which is equal to $K\cdot s_m$. K is the proportion coefficient can be defined by experimental condition.

$$F = \iint dF = \iint p\cdot\sin\beta\cdot\cos\gamma\cdot R^2\cdot\sin\beta\cdot d\beta d\gamma + \iint s\cdot\sin\gamma\cdot R^2\cdot\sin\beta\cdot d\beta d\gamma$$
$$= 2pR^2\int_0^\theta \sin^2\beta d\beta\int_0^{\pi/2}\cos\gamma d\gamma + 2sR^2\int_0^\theta \sin\beta d\beta\int_0^{\pi/2}\sin\gamma d\gamma \qquad 10$$
$$= pR^2(\theta - \sin\theta\cdot\cos\theta) + 2sR^2(1-\cos\theta)$$

Where, $\sin\theta = W/2R$, $\theta = \sin^{-1}(W/2R)$, $\csc^2\theta = (2R/W)^2$, $\cos\theta = [1-(W/2R)^2]^{1/2}$

The friction coefficient equation is obtained, by dividing equation 11 by equation 10, as:

$$\mu = \frac{F}{L} = \cdot\frac{2}{\pi}\left(\frac{2R}{W}\right)^2\left\{\sin^{-1}\left(\frac{W}{2R}\right) - \left(\frac{W}{2R}\right)\left[1-\left(\frac{W}{2R}\right)^2\right]^{1/2} + \frac{2}{N}\left(\frac{s}{s_m}\right)\left\{1-\left[1-\left(\frac{W}{2R}\right)^2\right]^{1/2}\right\}\right\} 11$$

Figure 7 shows the friction curves obtained from equation 11, assuming $N = 6$ [16], as a function of the ratio $W/2R$ for different interfacial frictional conditions.
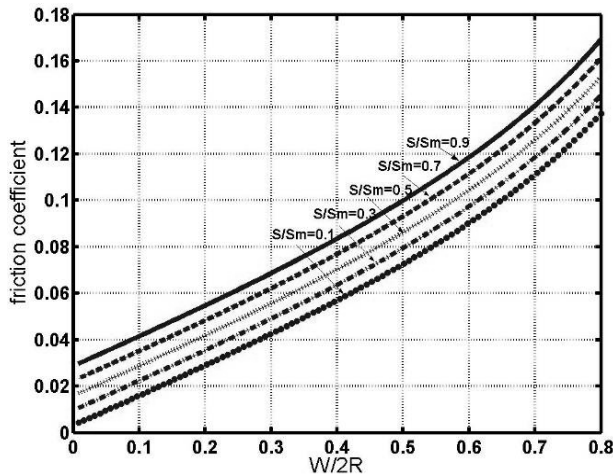

Fig. 7. Coefficient of boundary friction curve.

It is observed that the results calculated is more than that obtained via experiments under higher speed conditions. The reason can be explained as part of the plough effect was weakened by the

hydrodynamic lubrication (Fig. 8). Due to the lubricated effect considered in boundary film strength, the wet condition is included in boundary and adhesion term in equation 11. Thus, it is reasonable to correct the plough term in 11 and the coefficient K that weaken the plough is add in the equation11, the final equation is shown as 12.
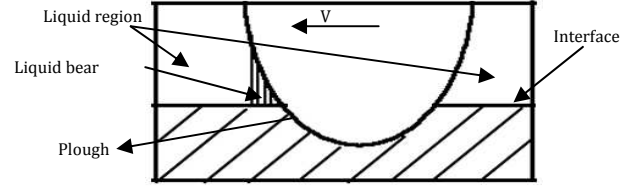

Fig. 8. Plough weakened by liquid under higher speed condition.

$$\mu = \frac{F}{L} = \frac{2}{\pi}\left(\frac{2R}{W}\right)^2\left\{k\cdot\left\{\sin^{-1}\left(\frac{W}{2R}\right) - \left(\frac{W}{2R}\right)\left[1-\left(\frac{W}{2R}\right)^2\right]^{1/2}\right\} + \frac{2}{N}\left(\frac{s}{s_m}\right)\left\{1-\left[1-\left(\frac{W}{2R}\right)^2\right]^{1/2}\right\}\right\} 12$$

Where μ is the friction coefficient, W is the interface diameter, R is the sphere radium, s is the interface shear stress, s_m is the body shear stress of softer material. s_l is the boundary film shear stress of interface. p is the pressure of unit. p_m is the hardness of the softer material and the $p = p_m$ generally. k is the weakened coefficient, k can be select from 0.1-0.8. N is the proportion coefficient assuming $N=6$. s is defined by the condition of the friction. $s = s_m$, in ideal dry friction condition. In ideal boundary friction condition, $s = s_l$. In general, s is between s_l and s_m.

3. RESULTS AND DISCUSSION

The friction model including plough and boundary effect is shown as equation 12. The results are shown as Fig. 7.

It shows that boundary friction coefficient is changing with the parameter ($W/(2R)$) and s/s_m. If the temperature of interface increasing, the bodies shear strength decrease meanwhile along with s/s_m increasing, the boundary friction coefficient increases. If the lubrication and cooling state is changed such as magnify the oil supply or use the oil with better absorption, the boundary friction coefficient would decline. The interface diameter W of friction plates in contact process is derived as:

$$W = \sqrt{R^2 - (R-\delta)^2} \qquad (13)$$

Thus, the boundary friction coefficient can be altered to the effects of deviation of the two surfaces, asperities radius and interface film strength together. The friction coefficient curve as a function of deviation of two surfaces is shown as Fig. 9. The friction coefficient is increasing and the friction coefficient sensitivity to deviation is decreasing along with the asperity curvature going up.
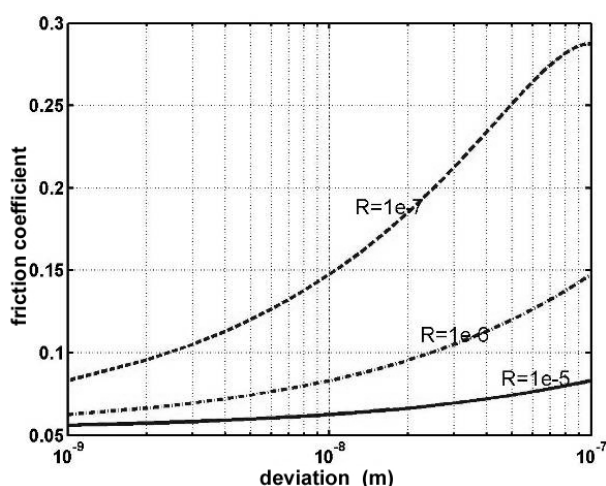

Fig. 9. Separation and boundary friction coefficient curve.

Fig. **10** shows the experimental devices in order to investigate the shear strength under various working conditions.

Fig. 10. Shear film strength testing device.

The s/s_m curves as a function of rotating speed can be obtained by the constant speed friction experimental device and shear strength test device (Fig. 10). It is observed that the adhesive

lock-up occurs when the relative rotating speed near 300r/min. Based on the analysis on the friction mechanism of four stages, assuming $s=s_m$ is reasonable when the relative rotating speed less than 300r/min for the experimental samples in the working condition listed in table 1. The s/s_m curves as a function of rotating speed show as Fig. 11.
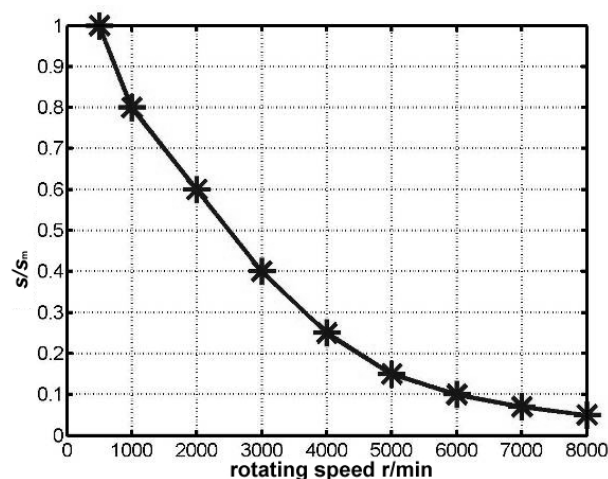

Fig. 11. Rotating speed and film strength curve.

The friction coefficient model considering the wet condition is derived as equation 12. The friction coefficient curve as a function of rotating speed is obtained by the fit curve via Fig. 11. In that most of the experiment was completed via braking process under heavy duty condition, the axis-x is reverse from high to low value. The sample was sintered bronze material and the size is $\Phi85*\Phi65$ (Fig. 12).

Fig. 12. Experiment sample.

The friction coefficient test experiments are performed on MM6000 friction and wear

experimental device (Fig. 13). The principle picture is shown as Fig. 14. The experimental is according to the method of JBT7909-1999 wet sintered friction material experimental testing.

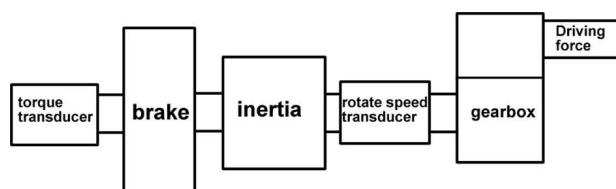**Fig. 13.** Experiment and device.

Fig. 14. The experimental principle picture.

The friction coefficient prediction curve as a function of rotating speed and different experimental data in three different pressures are both shown as Fig. 15 where $W/(2R) = 0.1$. As shown in Fig. 15, first, the friction coefficient increases along with the rotating speed declines. The main factor is that the interface film shear strength is improved due to the part of adhesion generated. Second, the friction coefficient is not sensitive to the pressure changed in the range from 0.5 MPa-1.5 MPa in that the pressure is not big enough to make friction mechanism changed and the pressure does not reach the critical value to rupture the boundary film.
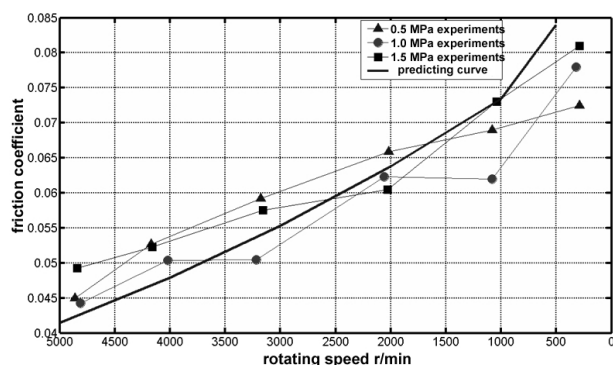

Fig. 15. Friction coefficient curve as a function of rotating speed.

4. CONCLUSION

The major conclusions of this investigation are as follows:

- The surface topography we observed by experiments verified the effect of plough cannot be neglected during engagement of friction plates.

- The friction state of wet clutch (brake) is different from dry friction. Account for the wet effect has considered in boundary term of the model, the weakening plough effect coefficient k was introduced to the plough term of friction coefficient model in order to simulate the wet condition effect.

- The interface film shear strength is improved due to the part of adhesion generated along with the body temperature going up. The friction coefficient is not sensitive to the pressure changed in the range from 0.5 MPa-1.5 MPa in that the pressure is not big enough to make friction mechanism changed and the pressure does not reach the critical value to rupture the boundary film.

- When the pressure range is form 0.5 MPa to 1.5 MPa, the higher the rotating speed, the smaller the friction coefficient in boundary friction stage during brake process for wet friction element. The agreement between theoretical and experimental friction coefficients is reasonably good.

Acknowledgement

REFERENCES

[1] W.B. Hardy and I. Doubleday: *Bounday Lubrication-The Paraffin Series*, in: *Proceedings of the Royal Society of London, Series A on Containing Papers of a Mathematical and Physical Character*, 01.03.1922, London, UK, pp. 550-574.

[2] F.P. Bowden, J.N. Georgey, D. Tabor: *Lubrication of metal surfaces by fatty acids*, Nature, Vol. 156, pp. 97-101, 1945.

[3] F.P. Bowden and D. Tabor: *The Friction and Lubrication of Solids*, Clarendon Press, Oxford 1958.

[4] K. Komvopoulos, N. Saka, N.P. Suh: *The mechanismof friction in boundary lubrication*, Journal of Tribology, Vol. 107, No. 11, pp. 452-462, 1985.

[5] H. Yoshizawa, Y.L. Chen, J. Israelachvili: *Fundamental mechanism of interfacial friction (relation between adhesion and friction)*, J. Phys. Chem., Vol. 97, pp. 4128–4140, 1993.

[6] G. Luengo, J. Israelachvili, S. Granick: *Generalized effects in confined fluids (new friction map for boundary lubrication),* Wear, Vol. 200, No. 1-2, pp. 328–335, 1996.

[7] G.J. Johnston, R. Wayte, H.A. Spikes: *The measurement and study of very thin lubricant films in concentrated contacts*, Tribology Transactions, Vol. 34, No. 2, pp. 187–194, 1991.

[8] M. Eguchi, T. Miyazaki, T. Yamamoto: *Boundary friction characteristic of wet friction materials (part 1, tangential displacement behavior under constant tangential loading conditions),* Journal of Japanese Society of Tribologists, Vol. 39, No. 2, pp. 160–167, 1994.

[9] M. Eguchi, T. Miyazaki, T. Yamamoto: *Boundary friction characteristic of wet friction materials (part 2, consideration on boundary friction–velocity characteristics by coefficient of tangential force–velocity relationship obtained under the conditions of constant tangential loading),* Journal of Japanese Society of Tribologists, Vol. 39, No. 2, pp. 168–175, 1994.

[10] F. Zivic, M. Babic, S. Mitrovic, P. Todorovic: *Interpretation of the Friction Coefficient During Reciprocating Sliding of Ti6Al4V Alloy Against Al2O3,* Tribology in Industry, Vol. 33, No. 1, pp. 36-42, 2011.

[11] M. Eguchi, T. Nakahara: *Friction–velocity characteristics of a paper-based wet friction material in low sliding velocity (part 1, boundary film model supposing eyring viscosity),* Journal of Japanese Society of Tribologists, Vol. 46, No. 2, pp. 162–170, 2001.

[12] T. Kugimiya: *Relationship between chemical structurese of dispersant and metallic detergent and m–v characteristics,* Journal of Japanese Society of Tribologists, Vol. 45, No. 5, pp. 396–405, 2000.

[13] W. Scott, P. Suntiwattana: *Effect of oil additives on the performance of a wet friction clutch material,* Wear, Vol. 181-183, No. 2, pp. 850-855, 1995.

[14] W.R.D. Wilson and S. Sheu: *Real Area of Contact and boundary Friction in Metal Forming*, International Journal of Mechanical Sciences, Vol. 30, No. 7, pp. 475-489, 1988.

[15] WANG Jiadao, CHEN Darong, KONG Xianmei, JI Kaiyuan: *Lubricating calculation for area contact of regular concave profiles*, Journal of Tsinghua University, Vol. 41, No. 2, pp. 42-45, 2001.

[16] J. Zhang, F.A. Moslehy and S.L. Rice: *A model for friction in quasi-steady-state sliding Part I. Derivation*, Wear, Vol. 149, No. 1-2, pp. 1-12, 1991.

[17] H. Czichos, D. Klaffke, E. Santner, M. Woydt: *Advances in tribology: the materials point of view*, Wear, Vol. 190, No. 2, pp. 155-161, 1995.